Phase space structures governing reaction dynamics in rotating molecules

Ünver Çiftçi[1,2] and Holger Waalkens[2]

[1] Department of Mathematics, Namık Kemal University, 59030 Tekirdağ, Turkey
[2] Johann Bernoulli Institute for Mathematics and Computer Science, University of Groningen, PO Box 407, 9700 AK Groningen, The Netherlands

E-mail: uciftci@nku.edu.tr and h.waalkens@rug.nl

Abstract

Recently, the phase space structures governing reaction dynamics in Hamiltonian systems have been identified and algorithms for their explicit construction have been developed. These phase space structures are induced by saddle type equilibrium points which are characteristic for reaction type dynamics. Their construction is based on a Poincaré–Birkhoff normal form. Using tools from the geometric theory of Hamiltonian systems and their reduction, we show in this paper how the construction of these phase space structures can be generalized to the case of the relative equilibria of a rotational symmetry reduced N-body system. As rotations almost always play an important role in the reaction dynamics of molecules, the approach presented in this paper is of great relevance for applications.

Mathematics Subject Classification: 70F10, 53C80, 37J25

PACS numbers: 45.50 Jf, 82.20.Nk, 45.20.Jj

(Some figures may appear in colour only in the online journal)

1. Introduction

From the perspective of dynamical systems theory a system shows reaction type dynamics if its phase space possesses a bottleneck type geometry. The system spends a long time in one phase space region before it finds its way through a bottleneck to another phase space region. In the terminology of chemistry these phase space regions correspond to 'reactants' and 'products', respectively, and the bottleneck connecting the two is called a 'transition state'. For Hamiltonian systems, the phase space bottlenecks result from equilibrium points of a certain stability type, namely equilibria for which the matrix associated with the linearization has one

791

pair of real eigenvalues of opposite sign and $f - 1$ complex conjugate pairs of imaginary eigenvalues, where f is the number of degrees of freedom. Such an equilibrium is called a saddle $\times$ centre $\times \cdots \times$ centre, and we will refer to them as 'saddle' for short. Near a saddle the energy surface (locally) bifurcates from an energy surface with two disjoint components (the reactants and products) for energies below the energy of the saddle to an energy surface consisting of a single connected component for energies above the energy of the saddle. The single component energy surface has a wide-narrow-wide geometry, and the system has to pass or 'react' through this bottleneck in order to evolve from reactants to products or vice versa. The most widely used approach to compute reaction rates in chemistry is to place a dividing surface in the bottleneck region and compute the rate from the flux through this dividing surface. This forms the basis of *Transition State Theory* that was developed by Eyring, Polanyi and Wigner in the 1930s [1, 2]. For this approach to be useful the dividing surface needs to have the property that it is crossed exactly once by all reactive trajectories (i.e. trajectories moving from reactants to products or vice versa) and not crossed at all by the non-reactive trajectories (i.e. trajectories staying on the reactants or products side). The construction of a dividing surface which solves this so-called recrossing problem has posed a major difficulty in the development of transition state theory. In the 1970s Pechukas, Pollak and others [3, 4] showed that for systems with two degrees of freedom, a recrossing free dividing surface can be constructed from a periodic orbit (the Lyapunov orbit associated with the saddle). The longstanding problem of how to generalize this idea for systems with more than two degrees of freedom has been solved only recently [5, 6], see also [7, 8]. Here the role of the Lyapunov orbit is taken over by a *normally hyperbolic invariant manifold* (NHIM) [9, 10] which forms the anchor for the construction of a dividing surface in the general case. The NHIM also gives a precise meaning of the transition state. It can be viewed as the energy surface of an invariant subsystem with $n - 1$ degrees of freedom, which as an unstable 'super molecule' [11] is located between reactants and products. The NHIM is not only of central significance for the construction of a recrossing free dividing surface, but also gives detailed information of the geometry and the mechanism of reactions. This arises from the fact that the NHIM has stable and unstable manifolds which are of one dimension less than the energy surface. They form the separatrices which separate the reactive trajectories and non-reactive trajectories in the energy surface. In fact, they form tubes which snake through the phase space and for a phase space point in the region of reactants to be reactive (i.e. for a point leading to a reactive trajectory if it is taken as an initial condition for Hamilton' s equations) it has to be contained in a certain volume that is enclosed by the stable manifold of the NHIM. Similarly, only points in the region of products can be reached by reactive trajectories emanating from the reactants if they are contained in a certain volume enclose by the unstable manifold of the NHIM. This information is crucial not only for the study of state specific reactivities but also for the control of reactions. Most importantly for applications, the dividing surface, the NHIM and the local pieces of its stable and unstable manifolds can be explicitly constructed from a Poincaré–Birkhoff normal form expansion about the saddle equilibrium point [6, 12]. The normal form gives a symplectic transformation to a new set of phase space coordinates in terms of which one can give simple formulas for the phase space structures. The inverse of the normal form transformation then allows one to construct the phase space structures in the original ('physical') coordinates.

In this paper, we address the question of how the phase space structures can be constructed for the relative equilibria of a rotational symmetry reduced N-body system. Here we have in mind that the N bodies represent the N atoms that constitute a given molecule (described in the Born–Oppenheimer approximation) but the theory presented also works for other N-body systems like celestial N-body systems. For molecular reactions, the excitation of rotational degrees of freedom almost always plays an important role. The phase space bottlenecks

are then no longer associated with equilibrium points but with larger sets of phase space points which however become again equilibria (so-called *relative equilbibria*) if considered in the rotational symmetry reduced system. In this context the reduction is important for both conceptual and computational reasons. We are particularly interested in a reduction which facilitates the Poincaré–Birkhoff normal construction of the phase space structures around a relative equilibrium in the same fashion as in the case of a usual saddle equilibrium. The theory of reduction for N-body systems is well developed [13–18]. However, although the structure of the reduced space is well known, the explicit choice of suitable coordinates for the reduced space remains as a challenging problem [19]. If the angular momentum is zero, the reduced space is symplectomorphic to the tangent bundle of the *shape* or *internal space* (see section 3). For non-vanishing angular momentum however, this is no longer the case [13]. This makes it difficult to apply classical techniques such as Poincaré–Birkhoff normal forms [20], and that point is the motivation of our paper (see also [21, 22]). A more canonical way of expressing the equations of motion is useful, and we hope that the theory presented in this paper will also be of interest for studies of N-body systems not only from the perspective of reaction dynamics but also from other perspectives. For relevant applications, we refer to [23–40].

In our approach we mainly follow the account given by Littlejohn and Reinsch [17]. Their reduction procedure can be viewed as a generalization of the free rigid body reduction scheme. Namely, the Hamiltonian is written as the sum of rotational kinetic energy, vibrational kinetic energy and the potential by passing to the body coordinates. The only remaining coordinates are the body angular momentum, the shape or internal coordinates and the conjugate momenta of the internal coordinates. However, using the body angular momentum the equations of motion have a non-canonical form which is not so suitable for the local analysis near equilibrium points [41–43]. Using the fact that the reduced space is locally a product of the body angular momentum sphere and the cotangent bundle of the internal space a canonical form of the equations of motions is obtained in this paper by choosing some suitable coordinates on the body angular momentum sphere.

This paper is organized as follows. In sections 2 and 3 we review the phase space structures governing reaction dynamics across saddle equilibrium points and the reduction of the rotational symmetry of N-body systems, respectively. The main result of this paper is contained in section 4 where we introduce a canonical coordinate system on the symmetry reduced space which facilitates Poincaré–Birkhoff normal form computations near equilibrium points. The theory is illustrated for the limiting case of a rigid body and the example of a triatomic molecule in section 5. Conclusions and an outlook are given in section 6.

2. Phase space structures governing reactions across saddles

In this section, we discuss the phase space structures governing reaction dynamics near saddle equilibrium points. Before studying the case of a general (nonlinear) Hamiltonian vector field it is useful to first consider the linear case. For the details we refer to [6, 12].

2.1. The linear case

Consider a linear Hamiltonian vector field with a saddle on the phase space $\mathbb{R}^f \times \mathbb{R}^f$ where $f \geqslant 2$ (we comment on the case $f = 1$ at the end of this section). Consider the quadratic Hamiltonian function

$$H_2(\boldsymbol{q}, \boldsymbol{p}) = \frac{\lambda}{2}(p_1^2 - q_1^2) + \sum_{k=2}^{f} \frac{\omega_k}{2}(p_k^2 + q_k^2). \tag{1}$$

The corresponding linear Hamiltonian vector field has a saddle equilibrium point at the origin, i.e. the matrix associated with the linear vector field has the pair of real eigenvalues $\pm\lambda$ and $f-1$ pairs of complex conjugate imaginary eigenvalues $\pm i\omega_k$, $k = 2, \ldots, f$. We define the constants of motion

$$\mathcal{I}_1 = \frac{p_1^2 - q_1^2}{2}, \qquad I_k = \frac{p_k^2 + q_k^2}{2}, \quad k = 2, \ldots, f, \tag{2}$$

which up to positive prefactors agree with the energies in the individual degrees of freedoms.

Consider a fixed energy $E > 0$, where 0 is the energy of the saddle. Rewriting the energy equation $H_2(\boldsymbol{q}, \boldsymbol{p}) = E$ in the form

$$\frac{\lambda}{2} p_1^2 + \sum_{k=2}^{f} \frac{\omega_k}{2}(p_k^2 + q_k^2) = E + \frac{\lambda}{2} q_1^2 \tag{3}$$

one sees that each fixed $q_1 \in \mathbb{R}$ defines a topological $(2f - 2)$-dimensional sphere. The energy surface

$$\Sigma_E = \{(\boldsymbol{q}, \boldsymbol{p}) \in \mathbb{R}^{2f} : H_2(\boldsymbol{q}, \boldsymbol{p}) = E\} \tag{4}$$

thus has the topology of a spherical cylinder $\mathbb{R} \times S^{2f-2}$. The 'radius' of the family of $(2f-2)$-dimensional sphere (3) becomes smallest for $q_1 = 0$, and this in fact can be used to define a recrossing free dividing surface (see the introduction). Setting $q_1 = 0$ on the energy surface gives the $(2f - 2)$-dimensional sphere

$$S_{\text{DS}}^{2f-2} = \{(\boldsymbol{q}, \boldsymbol{p}) \in \mathbb{R}^{2f} : H_2(\boldsymbol{q}, \boldsymbol{p}) = E, q_1 = 0\}. \tag{5}$$

The dividing surface S_{DS}^{2f-2} divides the energy surface into the two components which have $q_1 < 0$ (the 'reactants') and $q_1 > 0$ (the 'products'), respectively, and as $\dot{q}_1 = \partial H_2/\partial p_1 = \lambda p_1 \neq 0$ for $p_1 \neq 0$ the dividing surface is everywhere transverse to the Hamiltonian flow except for the submanifold where $q_1 = p_1 = 0$. For $q_1 = p_1 = 0$, the energy equation (3) reduces to $\sum_{k=2}^{f} \frac{\omega_k}{2}(p_k^2 + q_k^2) = E$. The submanifold thus is a $(2f - 3)$-dimensional sphere which we denote by

$$S_{\text{NHIM}}^{2f-3} = \{(\boldsymbol{q}, \boldsymbol{p}) \in \mathbb{R}^{2f} : H_2(\boldsymbol{q}, \boldsymbol{p}) = E, q_1 = p_1 = 0\}. \tag{6}$$

This is a so-called *normally hyperbolic invariant manifold* [9, 10] (NHIM for short), i.e. S_{NHIM}^{2f-3} is invariant (since $q_1 = p_1 = 0$ implies $\dot{q}_1 = \dot{p}_1 = 0$) and the contraction and expansion rates for motions on S_{NHIM}^{2f-3} are dominated by those components related to directions transverse to S_{NHIM}^{2f-3}. The NHIM (6) can be considered to form the equator of the dividing surface (5) in the sense that it divides it into two hemispheres which topologically are $(2f - 2)$-dimensional balls. All forward reactive trajectories (i.e. trajectories moving from reactants to products) cross one of these hemispheres, and all backward reactive trajectories (i.e. trajectories moving from products to reactants) cross the other of these hemispheres. Note that a trajectory is reactive only if it has $\mathcal{I}_1 > 0$ (i.e. if it has sufficient energy in the first degree of freedom). Trajectories with $\mathcal{I}_1 < 0$ are non-reactive, i.e. they stay on the side of reactants or on the side of products.

Due to its normal hyperbolicity the NHIM has stable and unstable manifolds which are given by setting $p_1 = -q_1$ resp. $p_1 = q_1$ on the energy surface. Each of them have two branches. We denote the branches of the stable manifold by

$$\begin{aligned}
W_{\text{NHIM;r}}^{\text{s}} &= \{(\boldsymbol{q}, \boldsymbol{p}) \in \mathbb{R}^{2f} : H_2(\boldsymbol{q}, \boldsymbol{p}) = E, \ p_1 = -q_1 > 0\}, \\
W_{\text{NHIM;p}}^{\text{s}} &= \{(\boldsymbol{q}, \boldsymbol{p}) \in \mathbb{R}^{2f} : H_2(\boldsymbol{q}, \boldsymbol{p}) = E, \ p_1 = -q_1 < 0\},
\end{aligned} \tag{7}$$

where W_r^s is located on the reactants side of the dividing surface and W_p^s is located on the product sides of the dividing surface. Similarly the unstable manifold has the two branches

$$W_{\text{NHIM};r}^u = \{(\boldsymbol{q}, \boldsymbol{p}) \in \mathbb{R}^{2f} : H_2(\boldsymbol{q}, \boldsymbol{p}) = E, \ p_1 = q_1 < 0\},$$
$$W_{\text{NHIM};p}^u = \{(\boldsymbol{q}, \boldsymbol{p}) \in \mathbb{R}^{2f} : H_2(\boldsymbol{q}, \boldsymbol{p}) = E, \ p_1 = q_1 > 0\}. \tag{8}$$

The stable and unstable manifolds have the topology of spherical cylinders $\mathbb{R} \times S^{2f-3}$. As they are of co-dimension 1 in the energy surface they can act as separatrices, dividing the energy surface into different components. In fact on the stable and unstable manifolds $\mathcal{I}_1$ is equal to zero. They thus lie 'between' the non-reactive ($\mathcal{I}_1 < 0$) and reactive ($\mathcal{I}_1 > 0$) trajectories. More precisely the forward reactive cylinder

$$C_f = W_{\text{NHIM};r}^s \cup W_{\text{NHIM};p}^u \tag{9}$$

encloses all forward reactive trajectories in the energy surface and separates them from all other trajectories, and similarly the backward reactive cylinder

$$C_b = W_{\text{NHIM};p}^s \cup W_{\text{NHIM};r}^u \tag{10}$$

encloses all backward reactive trajectories in the energy surface and separates them from all other trajectories. In this sense C_f and C_b form the phase space conduits of forward and backward reactions, respectively [44].

Moreover, it is useful to define the lines

$$\text{DRP}_f = \{(\boldsymbol{q}, \boldsymbol{p}) \in \mathbb{R}^{2f} : H_2(\boldsymbol{q}, \boldsymbol{p}) = E, \ p_1 > 0, \ p_k = q_k = 0, \ k = 2, \ldots, f\},$$
$$\text{DRP}_b = \{(\boldsymbol{q}, \boldsymbol{p}) \in \mathbb{R}^{2f} : H_2(\boldsymbol{q}, \boldsymbol{p}) = E, \ p_1 < 0, \ p_k = q_k = 0, \ k = 2, \ldots, f\}. \tag{11}$$

These lines form the centerlines of the volumes enclosed by the forward and backward reactive cylinders C_f and C_b, respectively, and are therefore referred to as the forward and backward dynamical reaction paths, respectively. All forward reactive trajectories spiral about DRP_f, and all backward reactive trajectories spiral about DRB_b. Note that in the limit $E \to 0^+$ the forward and backward reactive cylinders C_f and C_b shrink to the forward and backward dynamical reaction paths, which in turn become the one-dimensional stable and unstable manifolds of the saddle equilibrium point in this limit. More precisely, if

$$W_{\text{saddle};r}^s = \{(\boldsymbol{q}, \boldsymbol{p}) \in \mathbb{R}^{2f} : H_2(\boldsymbol{q}, \boldsymbol{p}) = 0, \ p_1 = -q_1 > 0, \ p_k = q_k = 0, \ k = 2, \ldots, f\},$$
$$W_{\text{saddle};p}^s = \{(\boldsymbol{q}, \boldsymbol{p}) \in \mathbb{R}^{2f} : H_2(\boldsymbol{q}, \boldsymbol{p}) = 0, \ p_1 = -q_1 < 0, \ p_k = q_k = 0, \ k = 2, \ldots, f\} \tag{12}$$

denote the reactants and product branches of the stable manifold of the saddle, and

$$W_{\text{saddle};r}^u = \{(\boldsymbol{q}, \boldsymbol{p}) \in \mathbb{R}^{2f} : H_2(\boldsymbol{q}, \boldsymbol{p}) = 0, \ p_1 = q_1 < 0, \ p_k = q_k = 0, \ k = 2, \ldots, f\},$$
$$W_{\text{saddle};p}^u = \{(\boldsymbol{q}, \boldsymbol{p}) \in \mathbb{R}^{2f} : H_2(\boldsymbol{q}, \boldsymbol{p}) = 0, \ p_1 = q_1 > 0, \ p_k = q_k = 0, \ k = 2, \ldots, f\} \tag{13}$$

denote the reactants and product branches of the unstable manifold of the saddle then $\text{DRP}_f \to W_{\text{saddle};r}^s \cup W_{\text{saddle};p}^u$ and $\text{DRP}_b \to W_{\text{saddle};p}^s \cup W_{\text{saddle};r}^u$ for $E \to 0^+$.

For systems with $f = 1$ degree of freedom with a saddle, one can still separate the phase space (or energy surface) in a reactants and a products region in a similar manner as described above. However, most of the phase space structures defined above make no sense for $f = 1$. The case of one degree of freedom is special since in this case the trajectories are given by the level sets of the Hamiltonian. The question of whether a trajectory is reactive or not is thus completely determined by the (total) energy of the trajectory.

2.2. The general (nonlinear) case

For the general nonlinear case, consider a Hamiltonian function H which has an equilibrium point (a 'saddle') at which the corresponding linearized vector field has the same disposition of eigenvalues as in section 2.1. In the neighbourhood of the saddle the dynamics is thus similar to that of the linear vector field described in section 2.1. In fact if follows from general principles that all the phase structures discussed in section 2.1 persist in the neighbourhood of the saddle (which in particular implies that one has to restrict to energies close to the energy of the saddle). Moreover, these phase space structures can be constructed in an algorithmic fashion using a Poincaré–Birkhoff normal form [6, 12]. Assuming that the eigenvalues ω_k, $k = 2, \ldots, f$, are independent over the field of rational numbers (i.e. in the absence of resonances), the Poincaré–Birkhoff normal form yields a symplectic transformation to new (*normal form*) coordinates such that the transformed Hamiltonian function truncated at order n_0 of its Taylor expansion assumes the form

$$H_{\mathrm{NF}}(\mathcal{I}_1, I_2, \ldots, I_f), \tag{14}$$

where $\mathcal{I}_1$ and I_k, $k = 2, \ldots, f$, are constants of motions which (when expressed in terms of the normal form coordinates) have the same form as in (2), and H_{NF} is a polynomial of order $n_0/2$ in $\mathcal{I}_1$ and I_k, $k = 2, \ldots, f$ (note that only even orders n_0 of a normal form make sense). The algorithm to compute this transformation is sketched in the appendix.

In terms of the normal form coordinates the phase space structures can be defined in a manner which is virtually identical to the linear case by replacing $H_2(\boldsymbol{q}, \boldsymbol{p})$ by $H_{\mathrm{NF}}(\mathcal{I}_1, I_2, \ldots, I_f)$ in the definitions in section 2.1. Using then the inverse of the normal form transformation allows one to construct the phase space structures in the original ('physical') coordinates. The Poincaré–Birkhoff normal form is therefore of crucial importance for the construction of the phase space structures governing reaction dynamics in a general Hamiltonian system with a saddle equilibrium point.

3. Reduction of the N-body system

We now want to study reaction type dynamics induced by the relative equilibria of a rotationally reduced N-body system. We start by recalling the reduction procedure for the N-body system following [17]. Let $\boldsymbol{x}_i$, $i = 1, \ldots, N$, be the position vectors of N bodies in $\mathbb{R}^3$. If a set of mass-weighted Jacobi vectors $\boldsymbol{s}_i$, $i = 1, \ldots, N-1$, are chosen (for an example, see section 5.2) and the centre of mass of the system is assumed to be the origin, then the three degrees of freedom associated with overall translations are eliminated, and the kinetic energy takes the diagonal form

$$K = \frac{1}{2} \sum_{i=1}^{N} \dot{\boldsymbol{s}}_i^2. \tag{15}$$

After a suitable choice of a body frame one can write $\boldsymbol{s}_i = \mathrm{R}(\theta_1, \theta_2, \theta_3)\boldsymbol{r}_i$ for some $\mathrm{R}(\theta_1, \theta_2, \theta_3) \in SO(3)$, where $\theta_1, \theta_2, \theta_3$ is some set of Euler angles, and $\boldsymbol{r}_i$, $i = 1, \ldots, N-1$, are the mass-weighted Jacobi vectors in the body frame. The $\boldsymbol{r}_i$ can be expressed in $3N - 6$ coordinates q_μ, called *shape* or *internal coordinates* and their space is called the *shape* or *internal space* which we denote by M. Away from collinear configurations, as we will assume throughout, the translation reduced space is a fibre bundle over the shape space. For a conservative N-body system without external forces the potential energy can be viewed as a function on the shape space (i.e. it is a function of the shape space coordinates only). The goal now is to also express the kinetic energy (as far as possible) as a function of the shape space coordinates. To this end we make the following definitions.

Let $R \in SO(3)$ denote the rotation from the centre of mass frame to the body frame and $\boldsymbol{L}$ denote the angular momentum

$$\boldsymbol{L} = \sum_{i=1}^{N} \boldsymbol{s}_i \times \dot{\boldsymbol{s}}_i. \tag{16}$$

Then the body velocities and body angular momentum are defined, respectively, by

$$\dot{\boldsymbol{r}}_i = R^T \dot{\boldsymbol{s}}_i, \tag{17}$$

and

$$\boldsymbol{J} = R^T \boldsymbol{L}. \tag{18}$$

The moment of inertia tensor $M(q)$ of the N-body system has the components

$$M_{ij}(q) = \sum_{k=1}^{N-1} (r_k^2 \delta_{ij} - r_{ki} r_{kj}), \tag{19}$$

where $\boldsymbol{r}_k = (r_{k1}, r_{k2}, r_{k3})$ in body coordinates. With the so-called *gauge potential*

$$\boldsymbol{A}_\mu(q) = M^{-1}(q) \cdot \sum_{i=1}^{N} \left(\boldsymbol{r}_i \times \frac{\partial \boldsymbol{r}_i}{\partial q_\mu} \right) \tag{20}$$

and the metric

$$g_{\mu\nu} = \frac{\partial r_\alpha}{\partial q_\mu} \frac{\partial r_\alpha}{\partial q_\nu} - \boldsymbol{A}_\mu \cdot M \cdot \boldsymbol{A}_\nu \tag{21}$$

(where we here and in the following use the Einstein convention of summation over repeated indices which run from 1 to $3N - 6$) the kinetic energy becomes

$$K = \tfrac{1}{2}(\omega + \boldsymbol{A}_\mu \dot{q}_\mu) \cdot M \cdot (\omega + \boldsymbol{A}_\nu \dot{q}_\nu) + \tfrac{1}{2} g_{\mu\nu} \dot{q}_\mu \dot{q}_\nu.$$

Here ω is the angular velocity which is the vector corresponding to the skew-symmetric matrix $R^T \dot{R}$ by the natural isomorphism

$$\begin{pmatrix} 0 & -\omega_3 & \omega_2 \\ \omega_3 & 0 & -\omega_1 \\ -\omega_2 & \omega_1 & 0 \end{pmatrix} \mapsto \begin{pmatrix} \omega_1 \\ \omega_2 \\ \omega_3 \end{pmatrix}. \tag{22}$$

Using the equation

$$\boldsymbol{J} = \frac{\partial K}{\partial \omega} = M(\omega + \boldsymbol{A}_\mu \dot{q}_\mu), \tag{23}$$

the conjugate momenta of the shape space coordinates are obtained by

$$p_\mu = \frac{\partial K}{\partial \dot{q}_\mu} = g_{\mu\nu} \dot{q}_\nu + \boldsymbol{J} \cdot \boldsymbol{A}_\mu. \tag{24}$$

The fully reduced Hamiltonian is then given by

$$H = \tfrac{1}{2} \boldsymbol{J} \cdot M^{-1} \cdot \boldsymbol{J} + \tfrac{1}{2} g^{\mu\nu}(p_\mu - \boldsymbol{J} \cdot \boldsymbol{A}_\mu)(p_\nu - \boldsymbol{J} \cdot \boldsymbol{A}_\nu) + V(q_1, \ldots, q_{3N-6}). \tag{25}$$

Here the first term is called *rotational* or *centrifugal energy* and the second one is called *vibrational kinetic energy*.

The equations of motion are obtained to be

$$\dot{q}_\mu = \partial H / \partial p_\mu, \qquad \dot{p}_\mu = -\partial H / \partial q_\mu, \qquad \dot{\boldsymbol{J}} = \boldsymbol{J} \times \frac{\partial H}{\partial \boldsymbol{J}} \tag{26}$$

for $\mu = 1, \ldots, 3N - 6$, [42]. The last equation is equivalent to [41]

$$\dot{J}_a = \{J_a, H\}, \qquad a = 1, 2, 3, \tag{27}$$

where $\boldsymbol{J} = (J_1, J_2, J_3)$.

The theory underlying the reduction described above is the orbit reduction method of Marle [45]. Let Q denote the translational reduced configuration space of non-collinear configurations. Then the action of $SO(3)$ on that space is free which implies that the lifted action of $SO(3)$ on T^*Q is also free in addition to being symplectic. The angular momentum can be considered as a map (a so called *momentum map*) J from T^*Q to the dual space of the Lie algebra of $SO(3)$, $\mathfrak{so}(3)^*$, which is identified with $\mathbb{R}^3$. After writing the Hamiltonian in terms of a body fixed frame, it takes an $SO(3)$-invariant form as in (25). As the (space fixed) angular momentum is constant, say ζ, and the modulus of the body angular momentum is also conserved, the dynamics can be reduced to the inverse image of the body angular momentum sphere $\mathcal{O}_\zeta = S^2_{\|\zeta\|}$ (which is the coadjoint orbit of the $SO(3)$ action) under the angular momentum map. Then (25) may be considered as a function on $J^{-1}(\mathcal{O}_\zeta)/SO(3)$ which is symplectomorphic to the Marsden–Weinstein space $J^{-1}(\zeta)/SO(2)$, where $SO(2)$ is the isotropy subgroup of the coadjoint action of $SO(3)$ on $\mathfrak{so}(3)^*$ [45].

4. Canonical coordinates on the reduced phase space

It can be seen by (25) that (q_μ, p_μ, J_a) are some coordinates on the reduced space where $\mu = 1, \ldots, 3N - 6$ and $J_a, a = 1, 2, 3$, are the components of the body angular momentum vector $\boldsymbol{J}$. Note here that (q_μ, p_μ) are canonical variables whereas the J_a are not canonical. If one uses coordinates $v_\mu = p_\mu - \boldsymbol{J} \cdot \boldsymbol{A}_\mu$ in place of p_μ, then (q_μ, v_μ) become non-canonical too [17] but this way it is easy to see that the reduced space is locally diffeomorphic to the product of the angular momentum sphere and the cotangent bundle of the internal space: $S^2_{\|\boldsymbol{J}\|} \times T^*M$. This is in fact a general fact for cotangent bundle reduction, known as *fibration cotangent bundle reduction* [45]. It is to be noted here that the symplectic structure on the reduced space is the sum of $\pm 1/\|\boldsymbol{J}\|$ times the volume form of the sphere, the canonical symplectic structure on T^*M and some magnetic terms [45]. The magnetic terms come from the gauge potential, and are directly related to the non-Euclidean structure of the shape space. The goal now is to use some canonical coordinates u, v on $S^2_{\|\boldsymbol{J}\|}$ instead of the coordinates J_a. The related symplectic structures on the coadjoint orbit S^2_r, where $r = \|\boldsymbol{J}\|$, are

$$w_\pm = \pm \frac{1}{r} \, \mathrm{d}A, \tag{28}$$

where $\mathrm{d}A$ is the volume form on the sphere. In terms of coordinates u, v the symplectic structure on S^2_r is

$$w_\pm = \pm \frac{1}{r} \sqrt{\det[g_{uv}]} \mathrm{d}u \wedge \mathrm{d}v, \tag{29}$$

where $[g_{uv}]$ is the matrix of the induced Riemannian metric on S^2_r by the Euclidean metric on $\mathbb{R}^3$. The canonical coordinates with respect to this symplectic structure are those that give
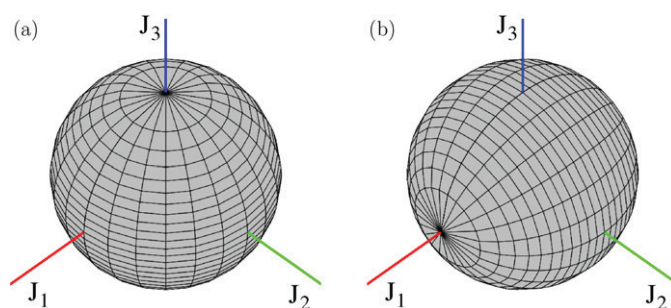
$$w_\pm = \pm \mathrm{d}u \wedge \mathrm{d}v.$$

One possible choice to achieve this is [46]

$$J_1 = \sqrt{r^2 - v^2} \cos u, \qquad J_2 = \sqrt{r^2 - v^2} \sin u, \qquad J_3 = v, \tag{30}$$

where $0 \leqslant u \leqslant 2\pi$, $-r \leqslant v \leqslant r$ (see figure 1(*a*)). Let u, v be some canonical coordinates for the positive signed symplectic structure w_+ and $q_\mu, p_\mu, 1 \leqslant \mu \leqslant 3N - 6$, be any choice of

Figure 1. (u, v) coordinate lines on the angular momentum sphere for (a) the definition of (u, v) in (30) and (b) the definition of (u, v) in (38).

shape coordinates and their conjugate momenta, respectively. In terms of these coordinates, after relabelling $u = q_0$, $v = p_0$, and setting $z = (z_i) = (q_i, p_i)$, $i = 0, \ldots, 3N - 6$, the equations of motion read

$$\dot{z}_i = \{z_i, H\} \tag{31}$$

or equivalently

$$\dot{q}_i = \partial H / \partial p_i, \qquad \dot{p}_i = -\partial H / \partial q_i \tag{32}$$

for $i = 0, \ldots, 3N - 6$, where the Poisson bracket on the reduced space has the standard form

$$\{f, g\} = \sum_{i=0}^{3N-6} \frac{\partial f}{\partial q_i} \frac{\partial g}{\partial p_i} - \frac{\partial f}{\partial p_i} \frac{\partial g}{\partial q_i}. \tag{33}$$

This canonical form of the equations of motion has many advantages. Although the coordinates p_μ, $\mu = 1, \ldots, 3N - 6$, are gauge dependent, for examining the local behaviour of the reduced system they can be used to study, for example, the stability of relative equilibria [41, 42]. We will use the canonical equations of motion to construct the phase space structures governing reaction type dynamics associated with saddle type relative equilbria in the reduced system from a Poincaré–Birkhoff normal form in the same way as described in section 2.

Relative equilibria are trivial solutions of the equations of motion (26) or equivalently (32). Using (26) one finds that the relative equilibria are the solutions of the reduced equations [42]

$$\boldsymbol{J} \times (\mathrm{M}^{-1} \cdot \boldsymbol{J}) = 0, \tag{34}$$

$$p_\mu = \boldsymbol{J} \cdot \boldsymbol{A}_\mu, \tag{35}$$

$$\frac{\partial}{\partial q_\mu}(\boldsymbol{J} \cdot \mathrm{M}^{-1} \cdot \boldsymbol{J} + V(q)) = 0. \tag{36}$$

This implies that at relative equilibria the body angular momentum $\boldsymbol{J}$ is parallel to a principal axis, i.e. the molecule is rotating about one of its principal axes. Using this fact the relative equilibria can be found from the critical points of the *effective potential*

$$V_{\mathrm{eff}}(q) = \boldsymbol{J} \cdot \mathrm{M}^{-1} \cdot \boldsymbol{J} + V(q), \tag{37}$$

where $\boldsymbol{J}$ is a fixed vector of a given modulus r parallel to a chosen principal axis. Some of these relative equilibria are related to the equilibria of the system with zero angular momentum. In fact for a triatomic molecule without any discrete symmetries, six families of relative equilibria are born out of any generic equilibrium if the modulus of the angular momentum is increased from zero. Here 'generic' means that the rotations act on the equilibrium configuration freely

(this excludes collinear configurations) [42]. We will follow this procedure to find relative equilibria in the example given in section 5.2.

Given a relative equilibrium we can determine its (linear) stability using the equations of motion (32). If the stability is of saddle type (as defined in the introduction) we can apply the Poincaré–Birkhoff normal form procedure described in the appendix to the equations of motion (32) in order to construct the phase structures governing reaction type dynamics as described in section 2. To this end we note that (u, v) defined as in (30) are singular at the north pole and south pole $\boldsymbol{J} = (0, 0, \pm r)$ of the angular momentum sphere. The coordinates are therefore not useful to study relative equilibria associated with rotations about the third principal axis [47]. In order to study these relative equilibria one can redefine (u, v) according to

$$J_1 = v, \qquad J_2 = \sqrt{r^2 - v^2} \sin u, \qquad J_3 = \sqrt{r^2 - v^2} \cos u \qquad (38)$$

in which case the coordinate singularities are at the points $\boldsymbol{J} = (0, \pm r, 0)$ on the angular momentum sphere (see figure 1(b)).

5. Examples

In the following we illustrate the approach above for the limiting case of a rigid molecule and the case of a triatomic molecule.

5.1. The limiting case of a rigid molecule

In the limiting case of a rigid molecule the internal degrees of freedom are frozen, i.e. $\dot{q}_\mu = \ddot{q}_\mu = 0, 1 \leqslant \mu \leqslant 3N - 6$. In this case, one can neglect the potential in (25) and the Hamiltonian reduces to

$$H = \tfrac{1}{2} \boldsymbol{J} \cdot \mathrm{M}^{-1} \cdot \boldsymbol{J} \qquad (39)$$

which describes the free rotation of a rigid body. Choosing the body frame to coincide with the principal axes, M (and its inverse M^{-1}) becomes diagonal and (39) becomes

$$H = \frac{1}{2} \left(\frac{J_1^2}{M_1} + \frac{J_2^2}{M_2} + \frac{J_3^2}{M_3} \right), \qquad (40)$$

where M_1, M_2 and M_3 are the principal moments of inertia. In this case the angular momentum part of (26) become the classical Euler equations [15]. In terms of the coordinates (u, v) defined in (30) these equations become
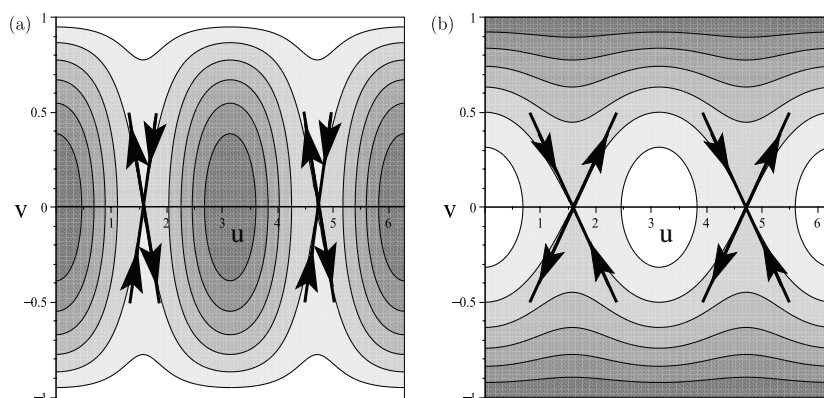
$$\dot{u} = \partial H / \partial v, \qquad \dot{v} = -\partial H / \partial u. \qquad (41)$$

Here the role of v is seen to be that of a momentum conjugate to v but when we choose the other symplectic form $\omega^- = -\frac{1}{r} \, \mathrm{d}A$ (see (28)), then the roles of u and v are reversed. If we choose the coordinates (30), then the Hamiltonian becomes

$$H(u, v) = \frac{1}{2} \left(\frac{(r^2 - v^2) \cos^2 u}{M_1} + \frac{(r^2 - v^2) \sin^2 u}{M_2} + \frac{v^2}{M_3} \right).$$

So, by (41) the equations of motion are obtained to be

$$\dot{u} = -\frac{v \cos^2 u}{M_1} - \frac{v \sin^2 u}{M_2} + \frac{v}{M_3},$$

$$\dot{v} = \frac{(r^2 - v^2) \sin u \cos u}{M_1} - \frac{(r^2 - v^2) \sin u \cos u}{M_2}.$$

Figure 2. Contours of the reduced rigid body Hamiltonian in the (u, v) coordinate plane with (u, v) defined according to (30) (a) and with (u, v) defined (38) (b). The energy increases from light to dark shading. The bold lines and arrows indicate the eigenvectors and the corresponding directions of the Hamiltonian flow for the saddles. The parameters are $M_1 = 1$, $M_2 = 2$, $M_3 = 3$ and $r = 1$.

In the case of the Euler top where the moments of inertia are mutually different, i.e. where we can assume without restriction that $M_1 < M_2 < M_3$, there are six relative equilibria given by the points $(\pm r, 0, 0)$, $(0, \pm r, 0)$ and $(0, 0, \pm r)$ on the J sphere. The dynamics near the first two can be studied in terms of the coordinates (u, v) defined according to (30) where they correspond to the points $(0, 0)$ (for $J = (r, 0, 0)$), $(\pi, 0)$ (for $J = (-r, 0, 0)$), $(\pi/2, 0)$ (for $J = (0, r, 0)$) and $(3\pi/2, 0)$ (for $J = (0, -r, 0)$) (see figure 2(a)). The dynamics near the relative equilibria $J = (0, 0, \pm r)$ (and again $J = (0, \pm r, 0)$) can be studied in terms of (u, v) defined according to (38) where they correspond to the points the points $(0, 0)$ (for $J = (0, 0, r)$), $(\pi, 0)$ (for $J = (0, 0, -r)$), $(\pi/2, 0)$ (for $J = (0, r, 0)$) and $(3\pi/2, 0)$ (for $J = (0, -r, 0)$) (see figure 2(b)). The reduced Hamiltonian has local maxima at $J = (\pm r, 0, 0)$ which correspond to rotations in either direction about the principal axis with the smallest moment of inertia, and minima at $J = (0, 0, \pm r)$ which correspond to rotations in either direction about the principal axis with the largest moment of inertia. The rotations about the principal axis with middle moment of inertia corresponding to $J = (0, \pm r, 0)$ are unstable. The corresponding relative equilibria are of saddle type. The eigenvalues associated with the linearized vector field are $\pm\sqrt{M_1 M 3(M_2 - M_1)(M_3 - M_2)}/(M_1 M_2 M_3)$. The eigenvectors are shown in figure 2. Since the reduced rigid body motion has one degree of freedom the reaction dynamics associated with these saddles is trivial (see the remarks at the end of section 2.1). One can divide the phase space of the reduced system into the regions $v < 0$ and $v > 0$ in terms of the coordinates (30) or equivalently in the regions $|u| < \pi/2$ and $|u| > \pi/2$ in terms of the coordinates (38) (where we used the periodicity of u in the last case; see figure 2). For energies below $r^2/(2M_2)$, which is the energy of the saddle, one cannot reach one region from the other. For energies above $r^2/(2M_2)$, however, this becomes possible.

5.2. Triatomic molecules: HCN

For a second example, we consider a triatomic molecule. We will use the so-called xxy gauge and Dragt's coordinates as follows [17]. Let x_1, x_3, x_3 be the position vectors of 3 bodies in

$\mathbb{R}^3$. If mass-weighted Jacobi vectors s_1, s_2 are chosen as

$$s_1 = \sqrt{\mu_1}(x_1 - x_3), \qquad s_2 = \sqrt{\mu_2}\left(x_2 - \frac{m_1 x_1 + m_3 x_3}{m_1 + m_3}\right), \tag{42}$$

where

$$\mu_1 = \frac{m_1 m_3}{m_1 + m_3} \qquad \text{and} \qquad \mu_2 = \frac{m_2(m_1 + m_3)}{m_1 + m_2 + m_3} \tag{43}$$

are the reduced masses then the corresponding Jacobi coordinates (ρ_1, ρ_2, ϕ) are defined by

$$\rho_1 = \|s_1\|, \qquad \rho_2 = \|s_2\|, \qquad s_1 \cdot s_2 = \rho_1 \rho_2 \cos\phi,$$

where $0 \leqslant \phi \leqslant \pi$. From the Jacobi coordinates one can define the coordinates

$$(w_1, w_2, w_3) = (\rho_1^2 - \rho_2^2, 2\rho_1\rho_2 \cos\phi, 2\rho_1\rho_2 \sin\phi), \tag{44}$$

where $w_1, w_2 \in \mathbb{R}$ and $w_3 \geqslant 0$. Dragt's coordinates (ω, χ, ψ) are now polar coordinates in the (w_1, w_2, w_3) coordinate space:

$$(w_1, w_2, w_3) = (\omega \cos\chi \cos\psi, \omega \cos\chi \sin\psi, \omega \sin\chi), \tag{45}$$

where $\omega > 0, 0 < \chi \leqslant \pi/2, 0 \leqslant \psi \leqslant 2\pi$. Note that ξ is the latitude, not the colatitude. The inertia and metric tensors are diagonal in Dragt's coordinates [17]:

$$M = \begin{bmatrix} \omega \sin^2 \frac{\chi}{2} & 0 & 0 \\ 0 & \omega \cos^2 \frac{\chi}{2} & 0 \\ 0 & 0 & \omega \end{bmatrix} \tag{46}$$

and

$$[g^{\mu\nu}] = \begin{bmatrix} 4\omega & 0 & 0 \\ 0 & \dfrac{4}{\omega} & 0 \\ 0 & 0 & \dfrac{4}{\omega \cos^2 \chi} \end{bmatrix}. \tag{47}$$

The gauge potential becomes

$$A_\omega = A_\chi = (0, 0, 0), \qquad A_\psi = (0, 0, -\tfrac{1}{2} \sin\chi). \tag{48}$$

Hence, if the coordinates (30) are used then after relabelling $u = q_0, v = p_0, \omega = q_1, \chi = q_2, \psi = q_3$, the reduced Hamiltonian becomes

$$H(q, p) = \frac{(r^2 - p_0^2) \cos^2 q_0}{2q_1 \sin^2 \frac{q_2}{2}} + \frac{(r^2 - p_0^2) \sin^2 q_0}{2q_1 \cos^2 \frac{q_2}{2}} + \frac{p_0^2}{2q_1} + 2q_1 p_1^2 + \frac{2p_2^2}{q_1} + \frac{(2p_3 + p_0 \sin q_2)^2}{2q_1 \cos^2 q_2}$$
$$+ V(q_1, q_2, q_3),$$

or if the coordinates (38) are used one has

$$H(q, p) = \frac{p_0^2}{2q_1 \sin^2 \frac{q_2}{2}} + \frac{(r^2 - p_0^2) \sin^2 q_0}{2q_1 \cos^2 \frac{q_2}{2}} + \frac{(r^2 - p_0^2) \cos^2 q_0}{2q_1} + 2q_1 p_1^2 + \frac{2p_2^2}{q_1}$$
$$+ \frac{(2p_3 + \sqrt{r^2 - p_0^2} \cos q_0 \sin q_2)^2}{2q_1 \cos^2 q_2} + V(q_1, q_2, q_3).$$

As a concrete example we consider the HCN molecule where we use the potential by Murrell *et al* [48]. The molecule exists in the form of two isomers which correspond to the
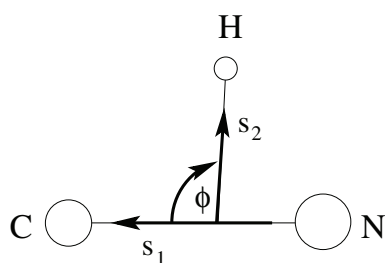
Figure 3. Definition of the Jacobi vectors s_1 and s_2 and the corresponding angle ϕ (see (42) and (5.2)) for the HCN molecule. Carbon is associated with the first mass, nitrogen is associated with the second mass and hydrogen is associated with the third mass.

collinear configurations HCN (hydrogen cyanide; the corresponding equilibrium has energy -13.5914 eV) and CNH (hydrogen isocyanide; the corresponding equilibrium has energy -13.1065 eV). For zero angular momentum, the reaction dynamics of the isomerization from HCN to CNH or vice versa is induced by a saddle equilibrium point which corresponds to a triangular (non-collinear) configuration (and has an energy of -12.0827 eV). The internuclear distances corresponding to this saddle are

$$d_{CN} = 1.1394 \,\text{Å}, \qquad d_{CH} = 1.1206 \,\text{Å}, \qquad d_{NH} = 1.4950 \,\text{Å}. \tag{49}$$

The eigenvalues of the matrix associated with the linearized vector field at this equilibrium are $\pm589.31\,\mathrm{i}$, $\pm418.69\,\mathrm{i}$ and ±213.08 (in units of inverse pico seconds) indicating that it is of saddle $\times$ centre $\times$ centre stability type.

We assign the Dragt's coordinates by identifying the first body with carbon, the second body with nitrogen and the third body with hydrogen (see figure 3). The internuclear distances are then given by

$$d_{CN} = \frac{1}{\sqrt{2\mu_1}} \sqrt{q_1 + q_1 \cos q_2 \cos q_3},$$

$$d_{CH} = \sqrt{\frac{\mu_1}{2m_1^2}(q_1 + q_1 \cos q_2 \cos q_3) + \frac{1}{2\mu_2}(q_1 - q_1 \cos q_2 \cos q_3) - \frac{\sqrt{\mu_1}}{m_1\sqrt{\mu_2}} q_1 \cos q_2 \sin q_3},$$

$$d_{NH} = \sqrt{\frac{\mu_1}{2m_3^2}(q_1 + q_1 \cos q_2 \cos q_3) + \frac{1}{2\mu_2}(q_1 - q_1 \cos q_2 \cos q_3) + \frac{\sqrt{\mu_1}}{m_3\sqrt{\mu_2}} q_1 \cos q_2 \sin q_3},$$

where m_1, m_2 and m_3 are the masses of carbon, nitrogen and hydrogen, respectively, and μ_1 and μ_2 are the reduced masses defined according to (43). The internuclear distances can also be viewed as coordinates on the shape space. The equipotential lines of the Murrell–Carter–Halonen potential intersected with the plane $d_{CN} = 1.1394$ (which contains the saddle) are shown in figure 4(a). In figure 4(a) also the projection of the eigenvectors corresponding to the real eigenvalues of the saddle are shown. Due to the time reversal symmetry of the system without angular momentum they project to the same line.

For the zero angular momentum saddle, the moment of inertia tensor has the diagonal elements [1.1645, 8.6470, 9.8115] (in the units of $\text{Å}^2 \times \text{eV}$). Due to the similar masses of carbon and nitrogen the values of the second and third moment of inertia are quite similar. We consider the six relative equilibria resulting from this saddle as the modulus r of the angular momentum is increased from zero (see section 4). Since the directions of rotations about either principal axis are related by symmetry there are effectively three families. We numerically compute these relative equilibria as a function of r from the critical points of the
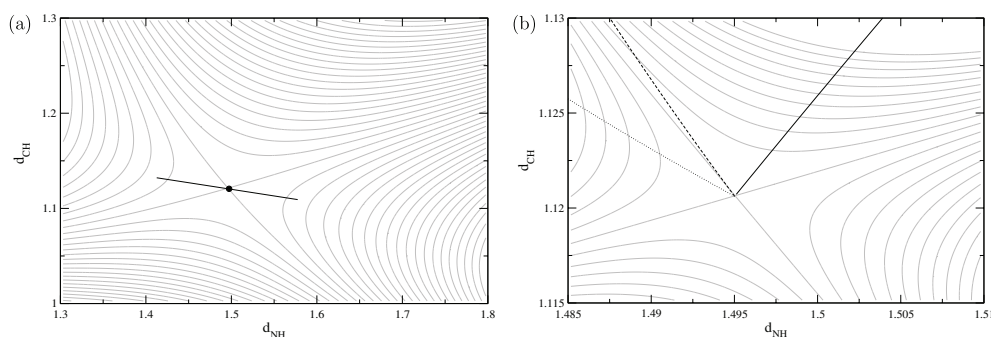
Figure 4. Potential energy lines (grey) of the Murrell *et al* [48] HCN potential in the section $d_{CN} = 1.1394$ Å together with (*a*) the projection of the real eigenvectors of the saddle equilibrium of the system with vanishing angular momentum and (*b*) the path traced by the relative equilibrium under variation of r projected to this plane for rotations about the first (full line), second (dashed line) and third (dotted line) principal axis.
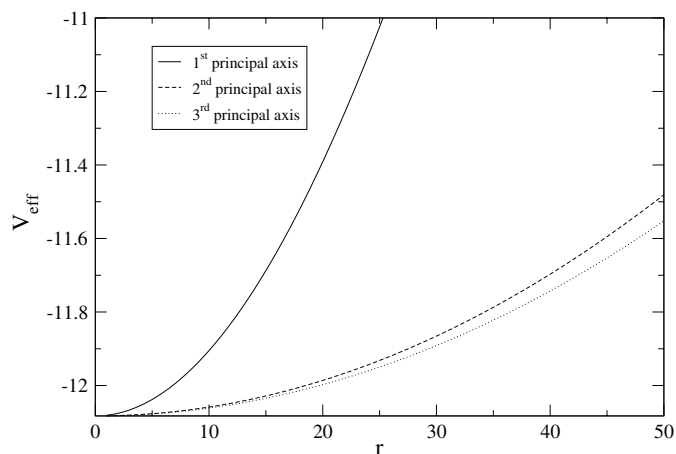
Figure 5. Energies of the relative equilibria as a function of the modulus of the angular momentum r. The energy is measured in eV and r is measured in units of $\hbar$. For fixed r, the relative equilibrium involving rotations about the principal axis with smallest (highest) moment of inertia has highest (smallest) energy.

effective potential $V_{\text{eff}}(q_1, q_2, q_3)$ in (37) where the angular momentum $\boldsymbol{J}$ is $(r, 0, 0)$, $(0, r, 0)$ or $(0, 0, r)$, respectively, using a Newton procedure. We show the energies of these relative equilibria as a function of r in figure 5. Since for a rigid body the rotation about the principal axis with middle moment of inertia is unstable, it is to be expected that, at least for small values of r, the two relative equilibria involving rotations about the first and the third principal axis are saddle $\times$ centre $\times$ centre $\times$ centres and the relative equilibrium involving rotations about the second principal axis is a saddle $\times$ saddle $\times$ centre $\times$ centre (which has two pairs of real eigenvalues and two complex conjugate pairs of imaginary eigenvalues). Linearizing the vector fields at the relative equilibria we find that this is indeed the case. In figure 6 we show the disposition of the eigenvalues in the complex plane as a function of r for the three cases. For $r \to 0$, the eigenvalues reduce in each case to the eigenvalues of the equilibrium in the system without angular momentum plus a double eigenvalue at zero.
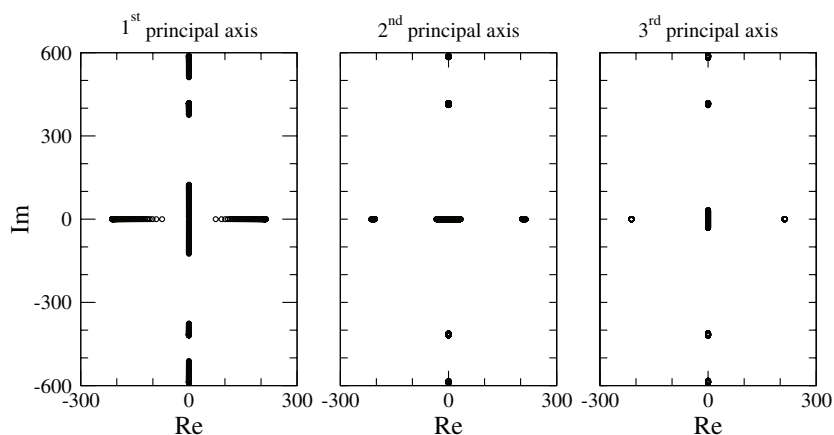
Figure 6. Paths traced by the eigenvalues (in units of inverse pico seconds) of the linearized vector fields as the modulus of the angular momentum r is varied for rotations about the first principal axis (left panel), the second principal axis (middle panel) and the third principal axis (right panel). The ranges for r are about the same as in figure 5.

Figure 4 shows the projections of the paths traced by the relative equilibria under variation of r to the (d_{CH}, d_{NH}) plane. One finds that in this projection the relative equilibrium corresponding to rotations about the first principal axis is moving much faster than the other two relative equilibria as r is varied. Note that the position of the relative equilibria on the angular momentum sphere does not change under variation of r.

The saddle type relative equilibria corresponding to rotations about the first and the third principal axis induce reaction type dynamics. The dynamics and its physical implications will be discussed in another publication. We here restrict ourselves to a brief discussion of the reaction paths in the limit where the energy approaches the energy of the relative equilibrium from above (see the discussion in section 2). In this limit the reaction paths reduce to the one-dimensional stable and unstable manifolds of the relative equilibria. At the relative equilibria these lines are tangent to the eigenvectors corresponding to the real eigenvalues of the linearization of the reduced system. We therefore show pictures of the pairs of real eigenvectors of the relative equilibria in figure 7. For the rotation about the first principal axis, the projections of the eigenvectors corresponding to positive and negative eigenvalues to the (d_{CH}, d_{NH}) plane are almost identical (similar to the angular momentum zero case). Their projections to the (u, v) plane, however, are quite different (see figures 7(a) and (b)). As the example indicates the relative equilibrium (in its projection to the shape space) might be quite far away from the position of the corresponding equilibrium of the system without angular momentum, and hence the reaction paths change quite considerably as a function of r. In the case of rotations about the third principal axis the projections of the eigenvectors of the two real eigenvalues to the (d_{CH}, d_{NH}) plane are quite different whereas their projections to the (u, v) plane is zero. The reason for the latter is related to the fact that in the case of rotation about the third principal axis the motion is planar (in the xxy gauge we are using the angular momentum vector is perpendicular to the plane spanned by the three bodies for rotations about the third principal axis). In figure 8 a piece of a trajectory reacting from HCN to CNH through the bottleneck induced by the relative equilibrium involving rotations about the third principal axis is shown. The trajectory has an angular momentum of modulus $r = 50\hbar$ and an energy of about 0.003 eV above the energy of the relative equilibrium. As indicated in figure 8(a) the Jacobi angle ϕ for the first part of the trajectory is oscillating between zero and about 1
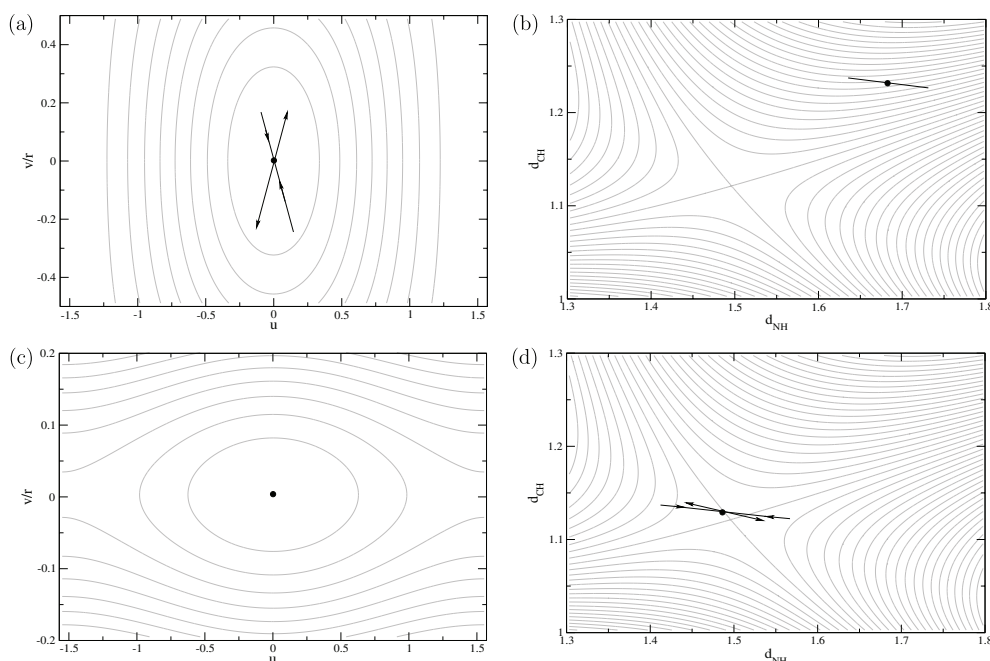
Figure 7. Saddle type relative equilibria and the corresponding real eigenvectors projected to the (u, v) plane and (d_{CH}, d_{NH}) plane, respectively for rotations about the first principal axis with $r = 33.5\,\hbar$ ((a) and (b)), and for rotations about the third principal axis with $r = 50\,\hbar$ ((c) and (d)).

which corresponds to rotational-vibrational motion of an HCN isomer (see figure 3) whereas after the isomerization reaction at about 0.5 ps the Jacobi angle ϕ is oscillating between about 1 and π which corresponds to the rotational-vibrational motion as a CNH isomer. Figure 8(b) shows the projection of the same piece of the trajectory to the (d_{CH}, d_{NH}) plane. One again sees the rotational-vibrational motion of the two isomers and the single transition between them. The inset in figure 8(b) shows the trajectory in the neighbourhood of relative equilibrium together with the real eigenvectors corresponding to the reaction in the direction from HCN to CNH. Note that the relatively small energy of 0.003 eV about the energy of the saddle relative equilibrium is still high enough to see oscillations transverse to the reaction path.

6. Conclusions and outlook

In this paper, we gave an explicit formalism to locally construct canonical coordinates in rotational symmetry reduced N-body systems. This allows one to study relative equilibria in such systems and use Poincaré–Birkhoff normal form to determine the phase space structures that govern reaction type dynamics near relative equilibria of saddle stability type. We briefly illustrated the formalism by applying it to the saddle relative equilibria which induce the isomerization reaction dynamics of HCN/CNH with rotation. Here, we restricted ourselves to the study of the reaction paths near the saddle relative equilibria. A more detailed study of the isomerization dynamics which includes a Poincaré–Birkhoff normal computation will be presented elsewhere. As an outlook we give a short list of open questions and future directions related to the work presented in this paper. A question that we did not discuss is the reconstruction problem, i.e. the study of what the corresponding motions of the reduced
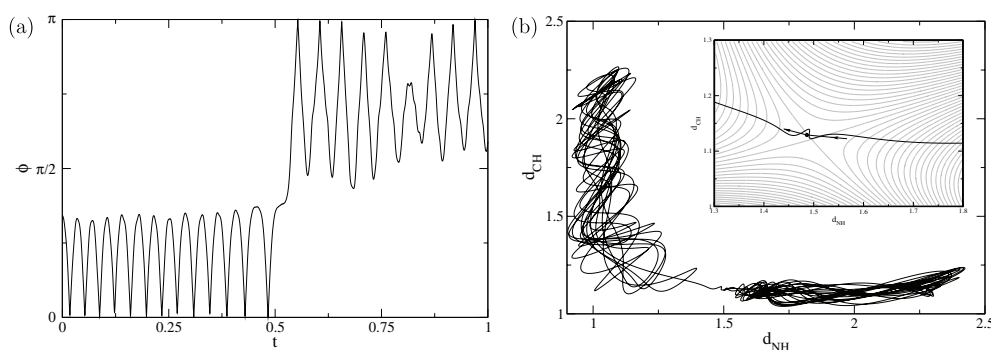
Figure 8. Piece of a reactive trajectory passing from HCN to CNH for $r = 50\hbar$ shown (a) as the Jacobi coordinate ϕ versus time t (in pico seconds) and (b) in the projection to the (d_{CH}, d_{NH}) plane. The inset in (b) shows a magnification of the part of the trajectory as it passes near the saddle relative equilibrium in figure 7(d). The trajectory has an energy of about -11.5498 eV.

system are in the full original system. In particular, from the perspective of reaction dynamics this is an interesting and important problem. The formalism introduced in this paper is not restricted to the study of relative equilibria of saddle type. Recently also the relevance of higher rank saddles for reaction type dynamics has been studied [49, 50]. In the HCN/CNH isomerization problem with angular momentum a saddle × saddle × centre × centre relative equilibrium (and its symmetric partner) is given by the rotation about the principal axis with the middle moment of inertia (and the two directions of rotation). Interestingly, for a fixed value of the modulus of the angular momentum, these rank 2 saddle relative equilibria are quite close in energy to the saddle relative equilibria corresponding to motion about the principal axis with the largest moment of inertia (see figure 5). It would be interesting to study the interplay between the phase space structures associated with the rank two saddles and usual saddles and their influence on the global dynamics. In [51–53] (see also [54]) a procedure based on transition state theory to determine the microcanonical volume of initial conditions that lead to reactive trajectories has been introduced. The formalism presented in this paper allows one to study such reactive volumes for rotational symmetry reduced systems. An interesting question for applications would be to study how this reactive volume changes when the modulus of the angular momentum is varied. The formalism presented in this paper at first only applies to relative equilibria of non-collinear configurations. We remark however that it can be quite simply adapted to also include collinear configurations. For this purpose, one can consider the Hamiltonian and coordinates in [42] and choose suitable coordinates in place of the angular momentum. In this paper we did not discuss the quantum reaction dynamics of rotating molecules. In [12, 55] the Weyl symbol calculus has been used to develop a quantum mechanical analogue of the Poincaré–Birkhoff normal form which provides an efficient procedure to compute quantum reaction rates and the related Gamov–Siegert resonances. The same procedure can, in principle, also be applied to the relative equilibria of rotational symmetry reduced molecules. However, the reduction of the quantum N-body system has some differences to the classical case. For example, for the quantum three-body problem one can separate rotations and vibrations whereas this is not possible in the classical case [56]. It would be very interesting to study the quantum reduction problem from the perspective of reaction dynamics. Finally we mention that shortly before the submission of our paper a related paper on the phase space structures governing reactions in rotating molecules was published [57]. That approach is based on a rovibrational Hamiltonian and its

Taylor expansion about a critical point of the potential using a rigid body approximation which is different from the approach in this paper where we start from an expansion about a relative equilibrium. Also the normalization procedure in [57] is different and in particular treats the body angular momentum in a non-canonical manner. It would be interesting to compare the two approaches.

Acknowledgments

Appendix. The normal form algorithm

Here we describe the algorithm to compute the Poincaré–Birkhoff normal form in the neighbourhood of a saddle equilibrium point of the form described in section 2.2. The implementation of this algorithm in a computer program is freely available [58].

Let H_2 denote the quadratic Hamiltonian which gives the linearized Hamiltonian vector field at the saddle. One says that a Hamiltonian H is in normal form if H Poisson commutes with its quadratic part, i.e.

$$\{H_2, H\} := \sum_{k=1}^{f} \left(\frac{\partial H_2}{\partial q_k} \frac{\partial H}{\partial p_k} - \frac{\partial H}{\partial q_k} \frac{\partial H_2}{\partial p_k} \right) = 0. \tag{50}$$

In general H is not in normal form. However, for any given order n_0 of the Taylor expansion of H one can find a symplectic transformation to new phase space coordinates in terms of which the transformed H truncated at order n_0 is in normal form. This symplectic transformation is constructed from a sequence of the form

$$(q_i, p_i) \equiv z \equiv z^{(0)} \mapsto z^{(1)} \mapsto z^{(2)} \mapsto z^{(3)} \mapsto \cdots \mapsto z^{(n_0)}, \tag{51}$$

where $z^{(n)}$ is obtained from $z^{(n-1)}$ by means of a symplectic transformation

$$z^{(n-1)} \mapsto z^{(n)} = \phi_{W_n} z^{(n-1)}. \tag{52}$$

generated by a polynomial $W_n(z)$ of order n, i.e.

$$W_n \in \mathcal{W}^n := \mathrm{span}\{q_1^{\alpha_1} \ldots q_f^{\alpha_f} p_1^{\beta_1} \ldots p_f^{\beta_f} : |\alpha| + |\beta| = n\}. \tag{53}$$

Here $|\alpha| = \sum_{k=1}^{f} \alpha_k$, $|\beta| = \sum_{k=1}^{f} \beta_k$. More precisely, the ϕ_{W_n} in (52) denote the time-one maps of the flows generated by the Hamiltonian vector fields corresponding to the polynomials W_n (see [12] for the details). The maximum order n_0 in (51) is the desired order of accuracy at which the expansion will be terminated and truncated.

Expressing the Hamiltonian H in the coordinates $z^{(n)}$, $n = 1, \ldots, n_0$, we obtain a sequence of Hamiltonians $H^{(n)}$,

$$H \equiv H^{(0)} \to H^{(1)} \to H^{(2)} \to H^{(3)} \to \cdots \to H^{(n_0)}, \tag{54}$$

where for $n = 1, \ldots, n_0$, $H^{(n)}(z^{(n)}) = H^{(n-1)}(z^{(n-1)}) = H^{(n-1)}(\phi_{W_n}^{-1} z^{(n)})$, i.e.

$$H^{(n)} = H^{(n-1)} \circ \phi_{W_n}^{-1}. \tag{55}$$

To avoid a proliferation of notation we will in the following neglect the superscripts (n) for the phase space coordinates.

In the first transformation in (51) we shift the equilibrium point z_0 to the origin, i.e. $z \mapsto \phi_{W_1}(z) := z - z_0$. This gives

$$H^{(1)}(z) = H^{(0)}(z + z_0). \tag{56}$$

The next steps of the normal form procedure rely on the power series expansions of $H^{(n)}$,

$$H^{(n)}(z) = E_0 + \sum_{s=2}^{\infty} H_s^{(n)}(z), \tag{57}$$

where the $H_s^{(n)}$ are homogenous polynomials in $\mathcal{W}^n$:

$$H_s^{(n)}(z) = \sum_{|\alpha|+|\beta|=s} \frac{H_{\alpha_1,\ldots,\alpha_f,\beta_1,\ldots,\beta_f}^{(n)}}{\alpha_1! \ldots \alpha_f! \beta_1! \ldots \beta_f!} q_1^{\alpha_1} \ldots q_f^{\alpha_f} p_1^{\beta_1} \ldots p_f^{\beta_f}. \tag{58}$$

For $n = 1$, the coefficients in (58) are given by the Taylor expansion of $H^{(1)}$ about the origin.

$$H_{\alpha_1,\ldots,\alpha_f,\beta_1,\ldots,\beta_f}^{(1)} = \prod_{k,l=1}^{f} \frac{\partial^{\alpha_k}}{\partial q_k^{\alpha_k}} \frac{\partial^{\beta_l}}{\partial p_l^{\beta_l}} H^{(1)}(z) \bigg|_{z=0}. \tag{59}$$

For $n \geqslant 3$, the coefficients in (58) are obtained recursively. For $n = 2$, i.e. the second step in the sequence of transformations (51), the coefficients in (58) are determined by a linear transformation of the phase space coordinates according to

$$z \mapsto \phi_{W_2}(z) := M z. \tag{60}$$

Here, M is a symplectic $2f \times 2f$ matrix which is chosen in such a way that the transformed Hamiltonian function

$$H^{(2)}(z) = H^{(1)}(M^{-1}z) \tag{61}$$

assumes the same form as in (1). Section 2.3 of [12] provides an explicit procedure for constructing the transformation matrix M.

For the first two steps in the sequence (51), we actually did not give explicit expressions for the generating functions W_1 and W_2. For conceptual reasons (and to justify the notation) it is worth mentioning that such expression can be determined (see [12]). The next steps in (51) though rely on the explicit computation of the generating functions W_n with $n \geqslant 3$. To this end it is convenient to introduce the adjoint operator associated with a phase space function A:

$$\mathrm{ad}_A : B \mapsto \mathrm{ad}_A B \equiv \{A, B\}. \tag{62}$$

The transformation (52) then leads to a transformation of the Hamilton function $H^{(n-1)}$ to $H^{(n)}$ with $n \geqslant 3$ which in terms of the adjoint operator reads

$$H^{(n)} = \sum_{k=0}^{\infty} \frac{1}{k!} [\mathrm{ad}_{W_n}]^k H^{(n-1)}. \tag{63}$$

In terms of the Taylor expansion defined in equations (57)–(59) the transformation introduced by equation (63) reads

$$H_s^{(n)} = \sum_{k=0}^{\lfloor \frac{s}{n-2} \rfloor} \frac{1}{k!} [\mathrm{ad}_{W_n}]^k H_{s-k(n-2)}^{(n-1)}, \tag{64}$$

where $\lfloor \cdot \rfloor$ gives the integer part of a number, i.e., the 'floor'-function.

Using equation (64) one finds that the transformation defined by (63) satisfies the following important properties for $n \geqslant 3$. Firstly, at step n, $n \geqslant 3$, the terms of order less than n in the power series of the Hamiltonian are unchanged, i.e.

$$H_s^{(n)} = H_s^{(n-1)}, \qquad \text{for } s < n, \tag{65}$$

so that, in particular, $H_2^{(n)} = H_2^{(2)}$. Defining

$$\mathcal{D} \equiv \mathrm{ad}_{H_2^{(2)}} = \{H_2^{(2)}, \cdot\} \tag{66}$$

we obtain for the term of order n,

$$H_n^{(n)} = H_n^{(n-1)} - \mathcal{D}W_n. \tag{67}$$

This is the so-called *homological equation* which will determine the generating functions W_n for $n \geqslant 3$ from requiring $\mathcal{D}H_n^{(n)} = 0$, or equivalently $H_n^{(n)}$ to be in the kernel of the restriction of $\mathcal{D}$ to $\mathcal{W}^n$. In view of (67) this condition yields

$$H_n^{(n-1)} - \mathcal{D}W_n \in \mathrm{Ker}\,\mathcal{D}|_{\mathcal{W}^n}. \tag{68}$$

Section 3.4.1 of [12] provides the explicit procedure of finding the solution of equation (68). In the generic situation where the linear frequencies $\omega_2, \ldots, \omega_f$ in (1) are rationally independent, i.e. $m_2\omega_2 + \cdots + m_f\omega_f = 0$ implies $m_2 = \ldots = m_f = 0$ for all integers $m_2, \ldots, m_f$, it follows that for odd n, $H_n^{(n)} = 0$, and for even n,

$$H_n^{(n)} \in \mathrm{span}\{\mathcal{I}^{\alpha_1} I_2^{\alpha_2} I_3^{\alpha_3} \ldots I_f^{\alpha_f} : |\alpha| = n/2\}, \tag{69}$$

where $\mathcal{I} = (p_1^2 - q_1^2)/2$ and $I_k = (q_k^2 + p_k^2)/2$, with $k = 2, \ldots, f$.

Applying the transformation (63), with the generating function defined by (67), for $n = 3, \ldots, n_0$, and truncating the resulting power series at order n_0 one arrives at the Hamiltonian $H_{\mathrm{NF}}^{(n_0)}$ corresponding to the n_0^{th} order *normal form* (NF) of the Hamiltonian H:

$$H_{\mathrm{NF}}^{(n_0)}(z) = E_0 + \sum_{s=2}^{n_0} H_s^{(n_0)}(z). \tag{70}$$

We stress that $H_{\mathrm{NF}}^{(n_0)}$ represents an n_0^{th} order approximation of the original Hamiltonian H obtained from expressing H in terms of the *normal form coordinates* z_{NF} which in turn are obtained from the symplectic transformation of the original coordinates $z = (q_i, p_i)$

$$z_{\mathrm{NF}} = \phi(z) = (\phi_{W_{n_0}} \circ \phi_{W_{n_0-1}} \circ \cdots \circ \phi_{W_2} \circ \phi_{W_1})(z). \tag{71}$$

This is why it is legitimate to use $H_{\mathrm{NF}}^{(n_0)}$ instead of H in analysing the dynamics in the neighbourhood of the saddle.

We emphasize that the full procedure to compute $H_{\mathrm{NF}}^{(n_0)}$ and the corresponding coordinate transformation is algebraic in nature, and can be implemented on a computer. A computer program is freely available from [58].

References

[1] Eyring H 1935 The activated complex in chemical reactions *J. Chem. Phys.* **3** 107–15
[2] Wigner E 1938 The transition state method *Trans. Faraday Soc.* **34** 29–48
[3] Pechukas P and McLafferty F J 1973 On transition-state theory and the classical mechanics of collinear collisions *J. Chem. Phys.* **58** 1622–5
[4] Pechukas P and Pollak E 1978 Transition states, trapped trajectories, and classical bound states embedded in the continuum *J. Chem. Phys.* **69** 1218–26
[5] Wiggins S, Wiesenfeld L, Jaffé C and Uzer T 2001 Impenetrable barriers in phase-space *Phys. Rev. Lett.* **86** 5478–81
[6] Uzer T, Jaffé C, Palacián J, Yanguas P and Wiggins S 2002 The geometry of reaction dynamics *Nonlinearity* **15** 957–92
[7] MacKay R S 1990 Flux over a saddle *Phys. Lett.* A **145** 425–7
[8] Komatsuzaki T and Berry R S 1999 Regularity in chaotic reaction paths: I. Ar$_6$ *J. Chem. Phys.* **110** 9160–73
[9] Wiggins S 1990 On the Geometry of transport in phase space: I. Transport in k-degree-of-freedom Hamiltonian systems, $2 \leqslant k \leqslant \infty$ *Physica* D **44** 471–501

[10] Wiggins S 1994 *Normally Hyperbolic Invariant Manifolds in Dynamical Systems* (Berlin: Springer)

[11] Pechukas P 1976 *Dynamics of Molecular Collisions* ed W H Miller (New York: Plenum)

[12] Waalkens H, Schubert R and Wiggins S 2008 Wigner's dynamical transition state theory in phase space: classical and quantum *Nonlinearity* **21** R1–R118

[13] Iwai T 1987 A geometric setting for classical molecular dynamics *Ann. Inst. Henri Poincaré Phys. Théor.* **47** 199–219

[14] Jellinek J and Li D H 1989 Separation of the energy of overall rotation in any N-body system *Phys. Rev. Lett.* **62** 241–4

[15] Marsden J E 1992 *Lectures on Mechanics* (*London Mathematics Society Lecture Note Series* vol 174) (Cambridge: Cambridge University Press)

[16] Kozin I N and Pavlichenkov I M 1996 Bifurcation in rotational spectra of nonlinear AB_2 molecules *J. Chem. Phys.* **104** 4105–113

[17] Littlejohn R G and Reinsch M 1997 Gauge fields in the separation of rotations and internal motions in the n-body problem *Rev. Mod. Phys.* **69** 213–75

[18] Iwai T and Tachibana A 1999 The geometry and mechanics of multi-particle systems *Ann. Inst. Henri Poincaré Phys. Théor.* **70** 525–59

[19] Roberts M, Schmah T and Stoica C 2006 Relative equilibria in systems with configuration space isotropy *J. Geom. Phys.* **56** 762–79

[20] Meyer K R and Hall G R 1992 *Introduction to Hamiltonian Dynamical Systems and the N-Body Problem* (Berlin: Springer)

[21] Pringle R Jr 1973 Satellite vibration-rotation motions studied via canonical transformations *Celestial Mech.* **7** 495–518

[22] Sahm D K, Weaver R V and Uzer T 1990 Depicting the intramolecular dynamics of formaldehyde *J. Opt. Soc. Am. B: Opt. Phys.* **7** 1865–74

[23] Churchill R C, Kummer M and Rod D L 1983 On averaging, reduction, and symmetry in Hamiltonian systems *J. Diff. Eqns* **49** 359–414

[24] Harter W G and Patterson C W 1984 Rotational energy surfaces and high-j eigenvalue structure of polyatomic molecules *J. Chem. Phys.* **80** 4241–61

[25] Elipe A and Ferrer S 1994 Reductions, relative equilibria, and bifurcations in the generalized van der Waals potential: relation to the integrable cases *Phys. Rev. Lett.* **72** 985–8

[26] Hanßmann H 1995 Normal forms for perturbations of the Euler top *Normal forms and homoclinic chaos (Waterloo, ON, 1992)* (*Fields Institute Communications* vol 4) (Providence, RI: American Mathematical Society) pp 151–173

[27] Miller M A 1996 Structure, rearrangements and evaporation of rotating atomic clusters *Mol. Phys.* **89** 533–54

[28] Sadovskií D 2001 Normal forms, geometry, and dynamics of atomic and molecular systems with symmetry *Symmetry and Perturbation Theory SPT 2001* ed M Cadoni *et al* pp 191–205

[29] Roberts M, Wulff C and Lamb J S W 2002 Hamiltonian systems near relative equilibria *J. Diff. Eqns* **179** 562–604

[30] Yurtsever E 2002 Measuring chaos in rotating clusters *Comput. Phys. Commun.* **145** 194–202

[31] Kozin I N and Roberts R M 2003 Monodromy in the spectrum of a rigid symmetric top molecule in an electric field *J. Chem. Phys.* **118** 10523–33

[32] Wiesenfeld L, Faure A and Johann T 2003 Rotational transition states: relative equilibrium points in inelastic molecular collisions *J. Phys. B: At. Mol. Phys.* **36** 1319–35

[33] Vera J A and Vigueras A 2006 Hamiltonian dynamics of a gyrostat in the n-body problem: relative equilibria *Celestial Mech. Dyn. Astron.* **94** 289–315

[34] Kozin I N, Sadovskií D A and Zhilinskií B I 2005 Assigning vibrational polyads using relative equilibria: application to ozone *Spectrochim. Acta* A **61** 2867–85

[35] Schmah T and Stoica C 2006 Stability for lagrangian relative equilibria of three-point-mass systems *J. Phys. A: Math. Gen.* **39** 14405–25

[36] Gurfil P, Elipe A, Tangren W and Efroimsky M 2007 The Serret-Andoyer formalism in rigid-body dynamics: I. Symmetries and perturbations *Regular Chaotic Dyn.* **12** 389–425

[37] Patrick G W, Roberts M and Wulff C 2008 Stability transitions for axisymmetric relative equilibria of Euclidean symmetric Hamiltonian systems *Nonlinearity* **21** 325–52

[38] Arango C A and Ezra G S 2008 Classical mechanics of dipolar asymmetric top molecules in collinear static electric and nonresonant linearly polarized laser fields: energy-momentum diagrams, bifurcations and accessible configuration space *Int. J. Bifurcation Chaos Appl. Sci. Eng.* **18** 1127–49

[39] Yanao T, Koon W S and Marsden J E 2009 Intramolecular energy transfer and the driving mechanisms for large-amplitude collective motions of clusters *J. Chem. Phys.* **130** 144111

[40] Chierchia L and Pinzari G 2011 The planetary N-body problem: symplectic foliation, reductions and invariant tori *Invent. Math.* **186** 1–77

[41] Kozin I N, Roberts R M and Tennyson J 1999 Symmetry and structure of rotating H_3^+ *J. Chem. Phys.* **111** 140–50

[42] Kozin I N, Roberts R M and Tennyson J 2000 Relative equilibria of D_2H^+ and H_2D^+ *Mol. Phys.* **98** 295–307

[43] Littlejohn R G and Mitchell K A 2002 Gauge theory of small vibrations in polyatomic molecules *Geometry, Mechanics, and Dynamics* (New York: Springer) pp 407–28

[44] Waalkens H, Burbanks A and Wiggins S 2004 Phase space conduits for reaction in multidimensional systems: HCN isomerization in three dimensions *J. Chem. Phys.* **121** 6207–25

[45] Ortega J-P and Ratiu T S 2004 *Momentum maps and Hamiltonian reduction* (Boston, MA: Birkhäuser)

[46] Deprit A 1967 Free rotation of a rigid body studied in the phase plane *Am. J. Phys.* **35** 424–8

[47] Cushman R H and Bates L M 1997 *Global Aspects of Classical Integrable Systems* (Basel: Birkhäuser)

[48] Murrell J N, Carter S and Halonen L O 1982 Frequency optimized potential energy functions for the ground-state surfaces of HCN and HCP *J. Mol. Spectrosc.* **93** 307–16

[49] Ezra G S and Wiggins S 2009 Phase-space geometry and reaction dynamics near index 2 saddles *J. Phys. A: Math. Gen.* **42** 205101

[50] Haller G, Uzer T, Palacián J, Yanguas P and Jaffé C 2011 Transition state geometry near higher-rank saddles in phase space *Nonlinearity* **24** 527–61

[51] Waalkens H, Burbanks A and Wiggins S 2005 Efficient procedure to compute the microcanonical volume of initial conditions that lead to escape trajectories from a multidimensional potential well *Phys. Rev. Lett.* **95** 084301

[52] Waalkens H, Burbanks A and Wiggins S 2005 A formula to compute the microcanonical volume of reactive initial conditions in transition state theory *J. Phys. A: Math. Gen.* **38** L759–68

[53] Waalkens H, Burbanks A and Wiggins S 2005 Escape from planetary neighbourhoods *Mon. Not. R. Astron. Soc.* **361** 763–75

[54] Ezra G S, Waalkens H and Wiggins S 2009 Microcanonical rates, gap times, and phase space dividing surfaces *J. Chem. Phys.* **130** 164118

[55] Schubert R, Waalkens H and Wiggins S 2006 Efficient computation of transition state resonances and reaction rates from a quantum normal form *Phys. Rev. Lett.* **96** 218302

[56] Iwai T 1987 A geometric setting for internal motions of the quantum three-body system *J. Math. Phys.* **28** 1315–26

[57] Kawai S and Komatsuzaki T 2011 Phase space geometry of dynamics passing through saddle coupled with spatial rotation *J. Chem. Phys.* **134** 084304

[58] Collins P, Burbanks A, Wiggins S, Waalkens H and Schubert R 2008 Bristol University normal form software http://lacms.maths.bris.ac.uk/publications/software